

## Variability of measured modal frequencies of a cable-stayed bridge under different wind conditions

Y. Q. Ni<sup>†</sup>, J. M. Ko<sup>‡</sup>, X. G. Hua<sup>††</sup> and H. F. Zhou<sup>‡‡</sup>

*Department of Civil and Structural Engineering, The Hong Kong Polytechnic University,  
Hung Hom, Kowloon, Hong Kong*

*(Received October 25, 2006, Accepted December 26, 2006)*

**Abstract.** A good understanding of normal modal variability of civil structures due to varying environmental conditions such as temperature and wind is important for reliable performance of vibration-based damage detection methods. This paper addresses the quantification of wind-induced modal variability of a cable-stayed bridge making use of one-year monitoring data. In order to discriminate the wind-induced modal variability from the temperature-induced modal variability, the one-year monitoring data are divided into two sets: the first set includes the data obtained under weak wind conditions (hourly-average wind speed less than 2 m/s) during all four seasons, and the second set includes the data obtained under both weak and strong (typhoon) wind conditions during the summer only. The measured modal frequencies and temperatures of the bridge obtained from the first set of data are used to formulate temperature-frequency correlation models by means of artificial neural network technique. Before the second set of data is utilized to quantify the wind-induced modal variability, the effect of temperature on the measured modal frequencies is first eliminated by normalizing these modal frequencies to a reference temperature with the use of the temperature-frequency correlation models. Then the wind-induced modal variability is quantitatively evaluated by correlating the normalized modal frequencies for each mode with the wind speed measurement data. It is revealed that in contrast to the dependence of modal frequencies on temperature, there is no explicit correlation between the modal frequencies and wind intensity. For most of the measured modes, the modal frequencies exhibit a slightly increasing trend with the increase of wind speed in statistical sense. The relative variation of the modal frequencies arising from wind effect (with the maximum hourly-average wind speed up to 17.6 m/s) is estimated to range from 1.61% to 7.87% for the measured 8 modes of the bridge, being notably less than the modal variability caused by temperature effect.

**Keywords:** cable-stayed bridge; structural health monitoring; modal variability; wind effect; temperature effect; correlation analysis.

---

### 1. Introduction

Structural health monitoring has become an increasingly accepted technology to diagnose structural health and conditions in civil engineering community (Pines and Aktan 2002, Ko and Ni 2005). The core of a structural health monitoring system is the diagnostic algorithms for detection of the presence, location, and extent of structural damage followed by evaluating the impact of the damage on structural

---

<sup>†</sup>Associate Professor, Corresponding author, E-mail: [ceyqni@polyu.edu.hk](mailto:ceyqni@polyu.edu.hk)

<sup>‡</sup>Chair Professor, E-mail: [cejmko@inet.polyu.edu.hk](mailto:cejmko@inet.polyu.edu.hk)

<sup>††</sup>Research Assistant, E-mail: [cexghua@polyu.edu.hk](mailto:cexghua@polyu.edu.hk)

<sup>‡‡</sup>Research Associate, E-mail: [cehfzhou@polyu.edu.hk](mailto:cehfzhou@polyu.edu.hk)

performance and safety. Among a variety of diagnostic algorithms, the vibration-based diagnosis methods, that use measured changes in dynamic features of a structure to infer structural damage or degradation, have been extensively investigated (Doebeling, *et al.* 1998, Sohn, *et al.* 2004). Most of these methods neglect the effects of environmental changes on dynamic characteristics of the underlying structure. In reality, however, civil structures are subject to varying environmental and operational conditions such as temperature, wind, and traffic. These environmental effects also cause changes in dynamic and modal properties, which may mask the changes caused by structural damage. It has been reported that the environmental effects were one of the main pitfalls limiting successful applications of modal-based damage diagnosis methods to real structures (Farrar and Jauregui 1998, Alampalli 2000, Pines and Aktan 2002). It is of paramount importance to characterize normal variability of modal parameters due to environmental effects and discriminate such normal variability from abnormal changes in modal parameters caused by structural damage. When the effects of normal environmental variations are well understood or quantified, it is possible to achieve reliable and accurate structural damage identification through incorporating the environmental effect models into the damage detection methodologies in either a statistical or deterministic way (Worden, *et al.* 2002, Kim, *et al.* 2003, Olson, *et al.* 2005, Wenzel, *et al.* 2005, Ko and Ni 2007, Zhou, *et al.* 2007).

Among various environmental and operational factors affecting modal parameters, the influence of temperature on modal properties has been extensively investigated using experimental and field measurement data (Robert and Pearson 1996, Abdel Wahab and De Roeck 1997, Farrar, *et al.* 1997, Cornwell, *et al.* 1999, Sohn, *et al.* 1999, Alampalli 2000, Lloyd, *et al.* 2000, Rohrmann, *et al.* 2000, Bolton, *et al.* 2001, Peeters and De Roeck 2001, Ko, *et al.* 2003, Londono and Lau 2003, Kim, *et al.* 2004, Ni, *et al.* 2005b, Xia, *et al.* 2006). These investigations indicated that temperature was the critical source causing modal variability. In addition, studies have shown that vehicle mass has very little influence on the modal parameters of large-scale bridges (Kim, *et al.* 2001, De Roeck and Maeck 2002, Zhang, *et al.* 2002). However, for long-span cable-supported bridges, the variation in wind conditions has been shown a major contributory to changes in modal properties because of the response-amplitude-dependent modal parameters and the aeroelastic coupling between wind and bridge (Abe, *et al.* 2000, Mahmoud, *et al.* 2001, Link, *et al.* 2002, Chen, *et al.* 2004). Most of the studies observed that the modal frequencies had a slight decrease with the increase of wind speed; however, all the studies did not take into consideration the separation of temperature-induced modal variability from wind-induced modal variability.

In this study, the effect of wind speed on modal frequencies in the cable-stayed Ting Kau Bridge is investigated by using the long-term monitoring data obtained under weak wind and typhoon conditions. A special effort is made to remove the temperature effect in evaluating wind-induced modal variability. One-year monitoring data from 45 accelerometers, 7 anemometers and 83 temperature sensors permanently installed on the bridge are used for this study. First, a total of 770-hour acceleration and temperature data obtained under weak wind conditions (hourly-average wind speed less than 2 m/s) during all four seasons are utilized to extract the modal frequencies and average temperatures at one-hour intervals, with which an artificial neural network (ANN) model is formulated for each vibration mode to characterize the temperature-frequency correlation. Then 155-hour monitoring data of acceleration, wind speed and temperature obtained under both weak wind and typhoon conditions during the summer are used to quantify the wind-induced modal variability. The effect of temperature on the measured modal frequencies is eliminated by normalizing these modal frequencies to a reference temperature with the use of the ANN models and the measured temperature data. The wind-induced modal variability is then quantitatively evaluated by correlating the normalized modal frequencies for each vibration mode with the wind speed

measurement data. Statistical analysis is conducted and linear regression models of variations in modal frequencies with wind speed are obtained. Hypothesis testing is performed to assess the significance of correlation in the regression models.

## 2. Acquisition of measurement data

### 2.1. Instrumentation system

The Ting Kau Bridge in Hong Kong, as shown in Fig. 1, is a multi-span cable-stayed bridge with three monoleg towers supporting two main spans of 448 and 475 m respectively and two side spans of 127 m each. After completing its construction in 1998, the bridge was instrumented with a long-term structural health monitoring system by the Highways Department of Hong Kong SAR Government (Wong 2004). This system consists of more than 230 sensors permanently installed on the bridge, including accelerometers, displacement transducers, strain gauges, anemometers, temperature sensors, weigh-in-motion sensors and a global positioning system.

A total of 83 temperature sensors have been installed at different locations of the bridge to measure: (i) steel-girder temperature, (ii) temperature inside concrete deck, (iii) temperature in tower legs, (iv) temperature in asphalt pavement, and (v) atmosphere temperature. Likewise, 24 uni-axial accelerometers, 20 bi-axial accelerometers and one tri-axial accelerometer (a total of 67 signal channels) have been installed on the deck of two main spans and two side spans, the longitudinal stabilizing cables, the top of the three towers, and the base of the central tower to measure dynamic characteristics of the bridge. A total of 7 anemometers have been installed to surveil wind environments around the bridge, of which four (ultrasonic-type anemometers) are located at the deck level and the other three (propeller-type anemometers) are located at tower top. The deployment of temperature sensors, anemometers and accelerometers on the bridge is illustrated in Fig. 1. The measurement data were acquired at sampling rates of 0.07, 2.56 and 25.6 Hz for temperature, wind and acceleration, respectively. One-year (the year of 1999) continuous measurement data covering a full cycle of in-service environmental conditions are used for this study.

### 2.2. Data used for temperature-frequency correlation analysis

The one-year monitoring data, after removing those likely to be abnormal, have been divided into two sets in this study. The first set includes 770-hour data which were obtained under weak wind conditions

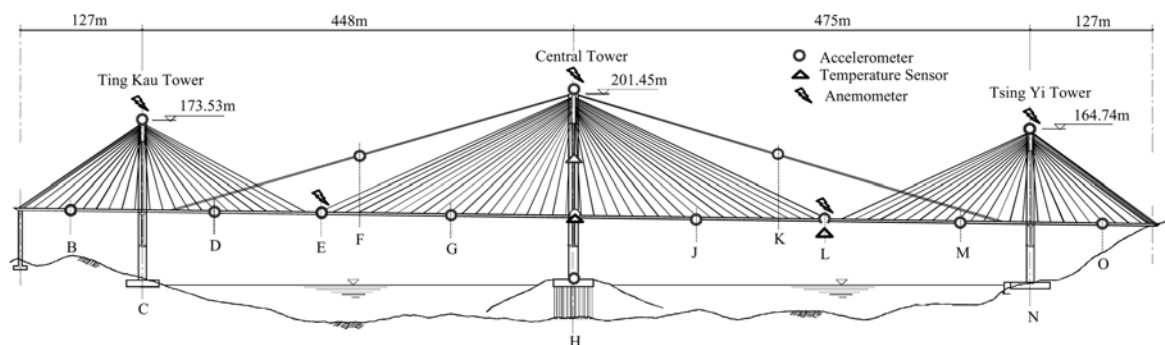


Fig. 1 Deployment of temperature sensors, anemometers and accelerometers on Ting Kau Bridge

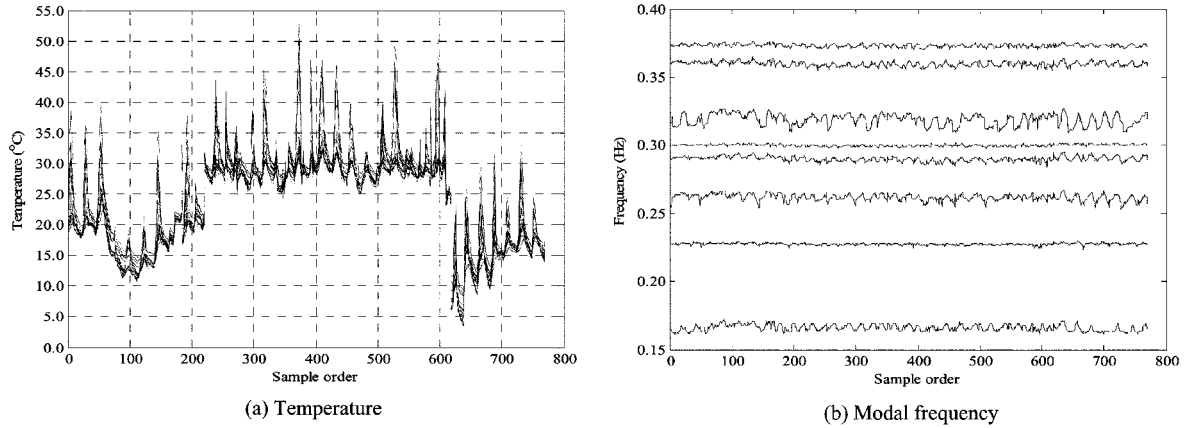


Fig. 2 Sequences of measured hourly-average temperatures and modal frequencies under weak wind conditions

(hourly-average wind speed less than 2 m/s) and from different seasons. It is composed of 185-hour data in February, 35-hour data in March, 95-hour data in June, 208-hour data in July, 95-hour data in August, and 152-hour data in December. With the acceleration measurement data, the natural frequencies and mode shapes of the first 8 vibration modes were identified at one-hour intervals by an automatic modal identification program (Ni, *et al.* 2005a). This program adopts the Complex Modal Indication Function (CMIF) algorithm and uses simultaneously all the measured data from 67 accelerometer channels for output-only modal identification. The measured temperatures were also hourly averaged. For the convenience of analysis, 4 sensors which are deployed at the locations most susceptible to temperature variation are selected from each of the five temperature monitoring categories. As a result, a total of 20 temperature sensors are chosen to provide measurement data for the temperature-frequency correlation analysis. Fig. 2 shows the sequences of the hourly-average temperatures from the 20 selected sensors and the measured modal frequencies for the first 8 modes.

Table 1 provides the statistics of the identified modal frequencies under weak wind conditions. The corresponding measured mode shapes refer to Ni, *et al.* (2005a). It is found that the first 8 modes lie in the frequency range of 0.1 to 0.4 Hz, indicating closely spaced modes in this bridge. For the identified 8

Table 1 Statistics of identified modal frequencies under weak wind conditions

Mode	Frequency range (Hz)	Average frequency (Hz)	Standard deviation ( $\times 10^{-3}$ Hz)	Variance (%)	Relative variation (%)
1st	0.150-0.175	0.1659	2.378	1.43	15.07
2nd	0.215-0.235	0.2273	0.783	0.34	8.80
3rd	0.245-0.275	0.2618	2.506	0.96	11.46
4th	0.275-0.305	0.2902	2.036	0.70	10.34
5th	0.290-0.308	0.2999	0.746	0.25	6.00
6th	0.305-0.335	0.3186	4.302	1.35	9.42
7th	0.340-0.370	0.3600	1.675	0.47	8.33
8th	0.369-0.381	0.3731	0.840	0.23	3.22

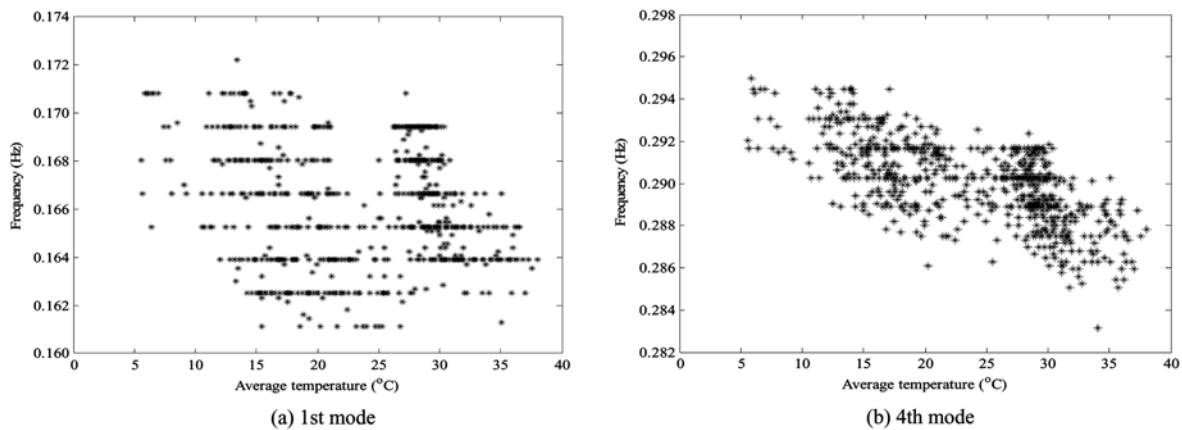


Fig. 3 Diagrams of modal frequency versus hourly-average temperature

modes, the relative variation of the measured modal frequencies (i.e. the ratio of frequency difference to average frequency for each mode) under weak wind conditions ranges from 3.22% (the 8th mode) to 15.07% (the 1st mode). The maximum relative variation (15.07%) is much larger than the observed temperature-induced frequency variability in general highway bridges. It is attributed to the fact that the cable-stayed Ting Kau Bridge has extremely low fundamental modal frequencies (its first modal frequency is even less than that of the world’s longest cable-stayed Tataru Bridge). The maximum absolute variation of the measured modal frequencies is 0.030 Hz only.

Fig. 3 illustrates the measured modal frequency versus the averaged temperature of those from the 20 sensors for the 1st and 4th modes, respectively. For all the measured modes, an overall decrease in modal frequency with the increase of temperature is observed. However, the temperature-frequency plotting is far from a linear pattern and highly dispersed. It implies that linear regression models should be incompetent for characterizing such a scattered relation. Hence, ANN technique will be used to formulate temperature-frequency correlation models.

### 2.3. Data used for wind-frequency correlation analysis

The second set of measurement data, which will be used for wind-frequency correlation analysis, was obtained under both weak wind and typhoon conditions during the summer. A total of 155-hour measurement data covering three typhoon events are included in the data set. As listed in Table 2, the maximum hourly-average wind speed measured at tower top is respectively 14.5, 14.1, and 17.6 m/s during the three typhoon events. With the 155-hour acceleration and temperature measurement data, the modal frequencies of the first 8 modes at one-hour intervals and hourly-average temperatures from the

Table 2 Durations covering three typhoon events

Typhoon	Time period of data	Duration (hours)	Maximum wind speed (m/s)
Leo	12:00 of 2 May to 05:00 of 4 May	42	14.5
Maggie	16:00 of 7 June to 08:00 of 9 June	41	14.1
Cam	00:00 of 25 September to 23:00 of 27 September	72	17.6

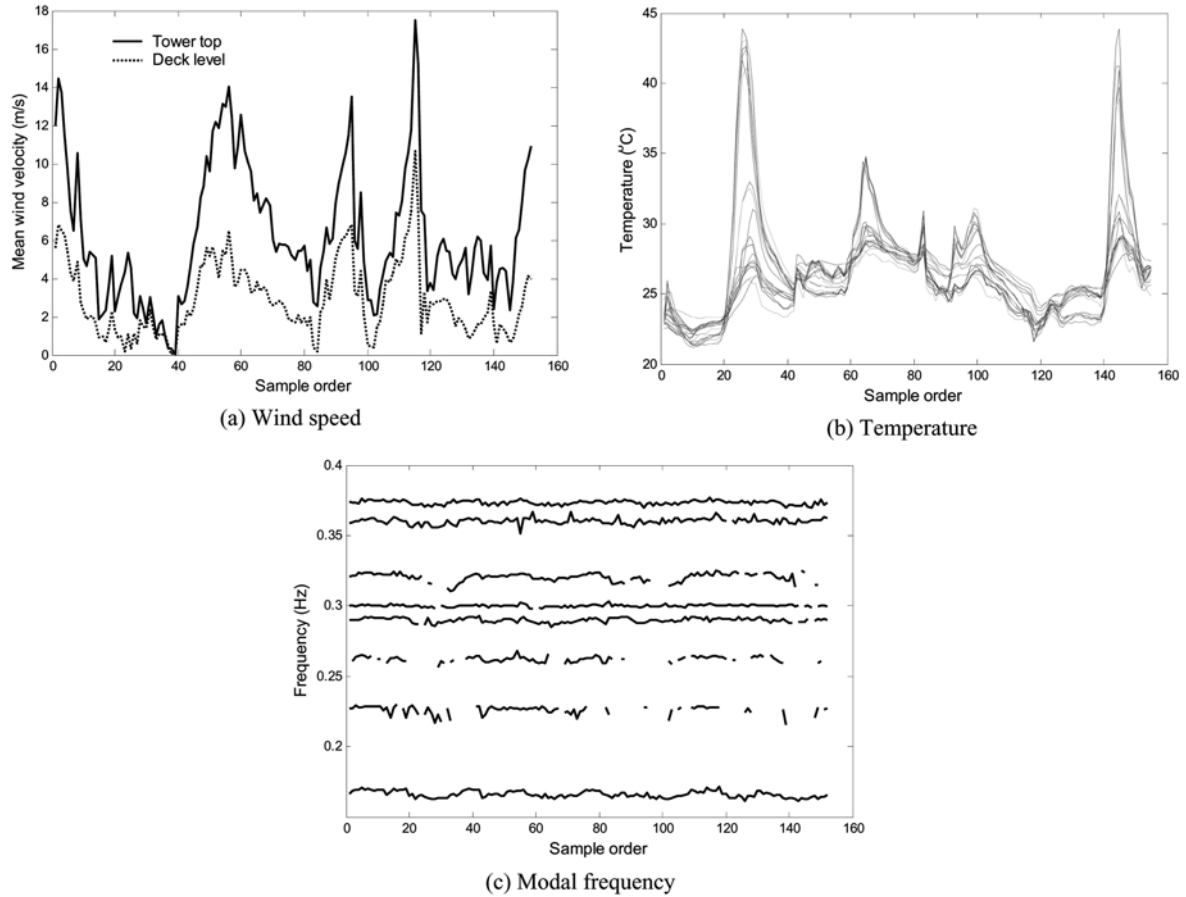


Fig. 4 Sequences of measured mean wind speeds, hourly-average temperatures and modal frequencies during three typhoon events

20 selected sensors are obtained following the same way as before. With the 155-hour wind measurement data, hourly-average wind speeds at deck level and tower top are obtained, respectively. The wind speed at deck level is obtained by averaging the data from the four anemometers installed on the deck, and the wind speed at tower top is obtained by averaging the data from the three anemometers installed at the top of towers. Fig. 4 illustrates the sequences of the hourly-average (mean) wind speeds at deck level and tower top, the hourly-average temperatures from the 20 sensors, and the measured modal frequencies for the first 8 modes. All the data will be used for modal frequency normalization and wind-frequency correlation analysis. Discontinuity in the modal frequency sequences as shown in Fig. 4(c) is due to the failure of modal identification for some time intervals in which the coupled torsional and lateral vibration modes of the bridge were not motivated.

### 3. Modeling of temperature-frequency correlation

As temperature is the critical source causing the variability in modal frequencies, it is necessary to remove the temperature effect on modal frequencies before the measurement data of modal frequencies

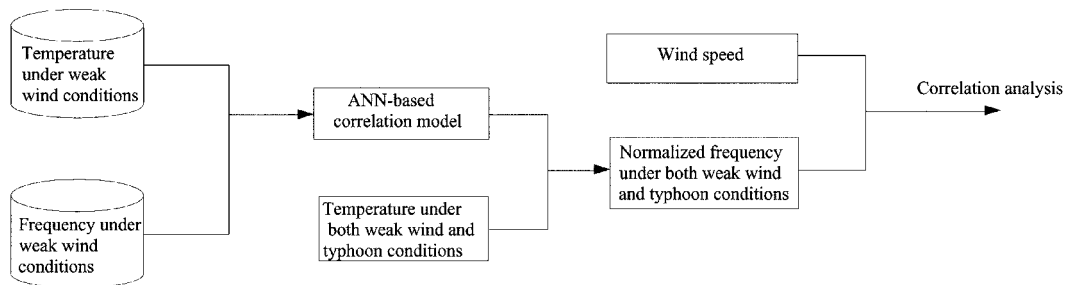


Fig. 5 Procedure for wind-induced modal variability analysis

and wind speeds are utilized for wind-frequency correlation analysis. Fig. 5 illustrates the proposed procedure for wind-induced modal variability analysis. By assuming that the modal frequencies obtained at low wind speeds are not affected by the variation in wind speeds, the measured modal frequencies and temperatures of the bridge under weak wind conditions (hourly-average wind speed less than 2 m/s) are selected to formulate temperature-frequency correlation models which will be used for eliminating the temperature effect in wind-frequency correlation analysis. ANN technique is applied herein for the modeling of temperature-frequency correlation.

### 3.1. Neural network topology

Among various ANN paradigms available, the feed-forward back-propagation (BP) neural network is by far the most widely utilized (Hegazy, *et al.* 1994, Adeli 2001). In this study, a BP neural network will be configured for each vibration mode for mapping between the temperatures and modal frequency. The input to the network is temperatures and the output is modal frequency. Since 20 temperature sensors have been selected to provide measurement data, the number of input nodes is set as 20. The output layer has only one node which represents the frequency at a specific mode. Because of no theoretical criterion, the number of hidden layers and the number of hidden nodes are determined through trial-and-error. Measurement data in a few months are first used as training and testing samples to try neural networks configured with different layer and node numbers. It is found that when using multiple hidden layers, the neural networks have excellent reproduction capability but are barely satisfactory in prediction. Instead, three-layer neural networks with appropriate hidden nodes are able to achieve satisfactory prediction performance and therefore adopted in this study. The hidden nodes of the three-layer neural networks are tried to be 6, 8, 10, 15, 20 and 25, and it is found that 10 hidden nodes are appropriate for all the modes. Three-layer neural networks with a node structure of 20-10-1 as shown in Fig. 6 are therefore employed for model formulation for all the 8 modes. The activation function is taken as the sigmoid function between the input and hidden layers and as a linear function between the hidden and output layers.

### 3.2. Modeling and results

In order to evaluate both the reproduction and generalization capabilities of the configured neural networks, the total 770-hour measurement data are alternately separated into two data sets: training samples and validation samples. For each mode, the training samples of both temperature and modal frequency are used to train the neural network. Then the training temperature samples are presented

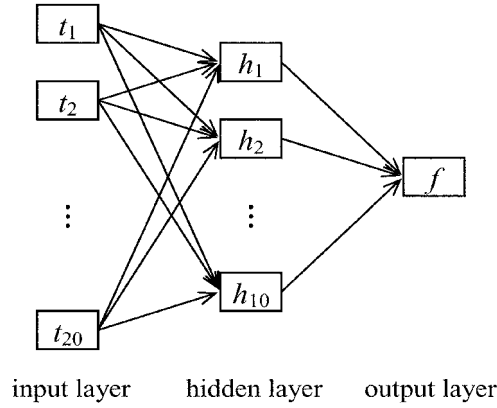


Fig. 6 Configuration of BP neural networks

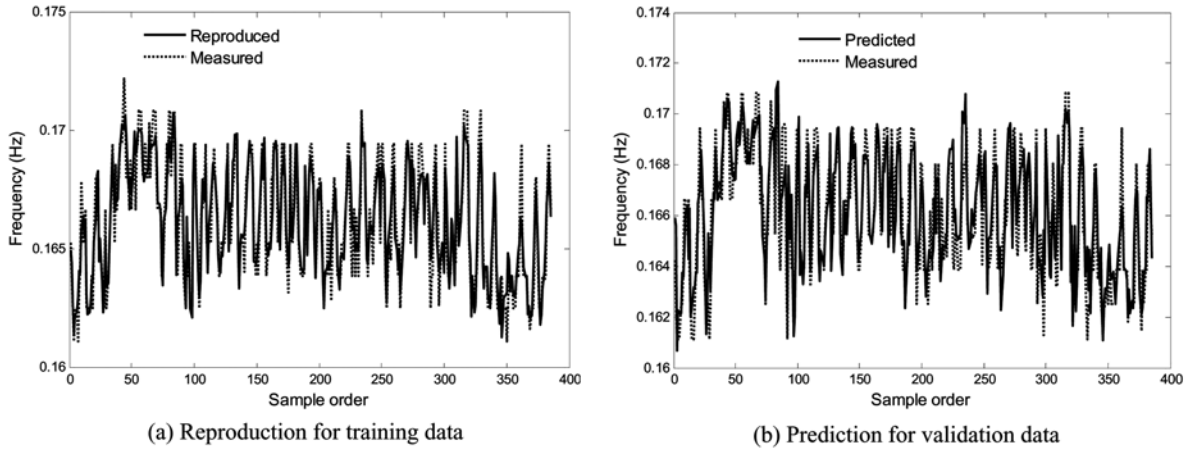


Fig. 7 Comparison between ANN-generated and measured frequencies for 1st mode

again as input into the trained network to generate frequency outputs which are compared with the target outputs (training frequency samples) to evaluate the reproduction (simulation) capability. Similarly, the validation temperature samples that were not used in the training are fed into the trained network to generate frequency outputs which are compared with the expected outputs (validation frequency samples) to evaluate the generalization (prediction) capability of the ANN model.

Figs. 7 and 8 show a comparison between the measured modal frequencies and those generated by the ANN models for training and validation data in the case of the 1st mode and the 4th mode, respectively. Both the reproduction and generalization capabilities of the formulated ANN models are validated. Table 3 summarizes the means and standard deviations of residuals of the reproduced frequencies associated with training samples and the predicted frequencies corresponding to testing samples for all the 8 modes. It is observed that the neural networks for all the 8 modes exhibit better reproduction (simulation) capability than generalization (prediction) capability, but the discrepancy is insignificant. The neural network for the 5th mode gives rise to the minimum residuals for both the reproduced and predicted frequencies, whereas the neural network for the 6th mode results in the maximum residuals

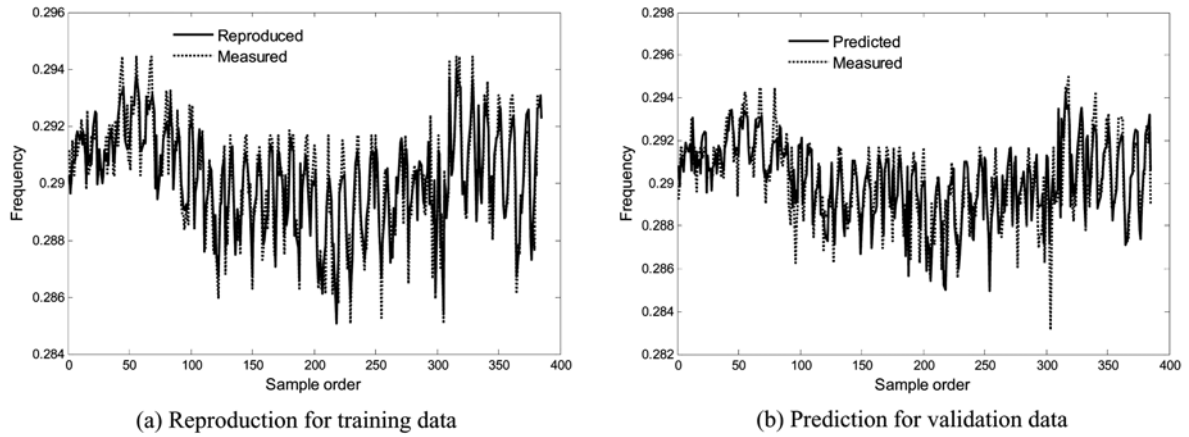


Fig. 8 Comparison between ANN-generated and measured frequencies for 4th mode

Table 3 Statistics of residuals of ANN-generated modal frequencies

Mode	Residuals of reproduced frequencies (Hz)		Residuals of predicted frequencies (Hz)	
	Mean ( $\times 10^{-4}$ )	Standard deviation ( $\times 10^{-3}$ )	Mean ( $\times 10^{-4}$ )	Standard deviation ( $\times 10^{-3}$ )
1st	0.0080	0.8906	1.6944	1.2522
2nd	0.0058	0.5127	-0.6459	0.6472
3rd	0.0084	0.8438	0.0790	1.5673
4th	-0.0021	0.6764	0.7090	1.0235
5th	-0.0016	0.4335	-0.3242	0.5823
6th	0.0012	1.2048	2.4102	2.0606
7th	0.0036	0.8955	0.0467	1.1820
8th	0.0049	0.7794	-0.3674	0.7860

for both the reproduced and predicted frequencies, indicating the consistence in simulation and prediction capabilities. It is worth mentioning that large residuals do not definitely imply poor simulation and prediction performance because the range of frequency variations caused by temperature effect is different for different modes as shown in Table 1. If a mode has a larger variation range in its measured frequencies than other modes, the residual deviation of the ANN-generated frequencies will be also larger for this mode than others under the identical simulation and prediction performance.

#### 4. Analysis of wind-induced modal variability

##### 4.1. Removal of temperature effect

Before the 155-hour measurement data obtained under both weak wind and typhoon conditions are used for wind-frequency correlation analysis, the temperature effect on the measured modal frequencies should be removed. It is achieved by normalizing all the measured frequencies to a set of fixed

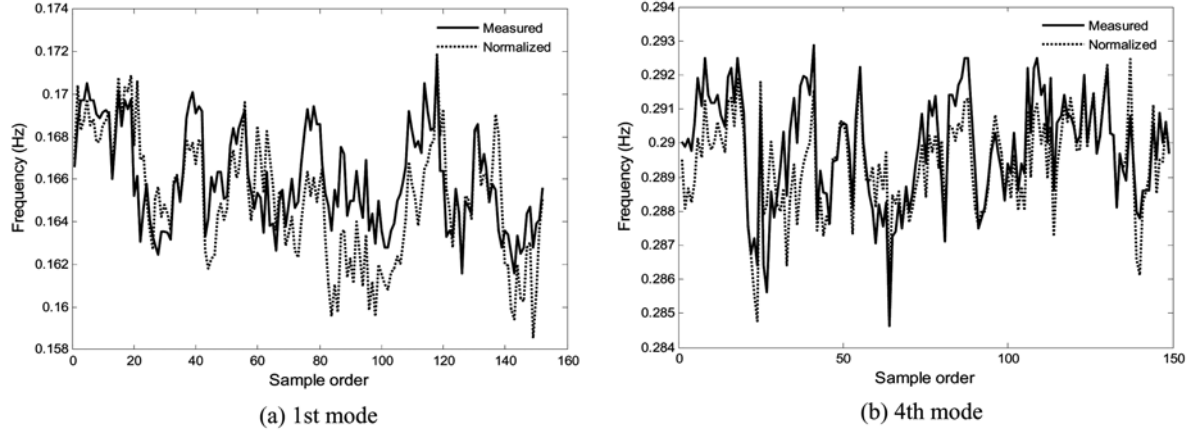


Fig. 9 Measured and normalized modal frequencies under weak wind and typhoon conditions

reference temperatures with the use of the established ANN models. In this study, the reference temperature for each temperature measurement point is taken as the average of the 770-hour measured temperatures used for training and validating the ANN models. By presenting the set of reference temperatures into the neural networks, a nominal frequency  $f_r$  is obtained for each mode. Likewise, by feeding the 155-hour temperature measurement data into the neural networks, a sequence of temperature-induced frequency variations  $f_{ii}$  ( $i = 1, 2, \dots, 155$ ) is predicted for each mode. Then the normalized modal frequencies after removing temperature effect are obtained by

$$f_i = f_{mi} - (f_{ii} - f_r) \quad (1)$$

where  $f_i$ 's are the normalized modal frequencies for each mode;  $f_{mi}$ 's are the measured modal frequencies for each mode; and subscript  $i$  ( $i = 1, 2, \dots, 155$ ) represents the sample order. It is known from Eq. (1) that a different choice of the reference temperature will result in an identical shift for all the normalized modal frequencies, which does not affect the correlation between the wind speed and the normalized modal frequency. Therefore, an arbitrary reference temperature can be adopted to obtain the normalized modal frequencies. For a specific temperature measurement point, a fixed value of the reference temperature should be used to normalize the measured modal frequencies obtained at different times (seasons).

Fig. 9 shows the measured and normalized modal frequencies for the 1st and 4th modes, respectively. The normalized modal frequencies, on which the temperature effect has been removed, will be used in conjunction with the wind measurement data obtained under weak wind and typhoon conditions for wind-frequency correlation analysis. Table 4 provides the statistics of the normalized modal frequencies. The change in the normalized modal frequencies is attributed to wind effect. By comparing the relative variations shown in Table 4 with those given in Table 1, it is concluded that the wind-induced modal variability is notably less than the temperature-induced modal variability.

#### 4.2. Wind-frequency correlation analysis

Correlation analysis is conducted on the normalized modal frequencies and the measured wind speeds under weak wind and typhoon conditions. Figs. 10 and 11 show the correlation diagrams of

Table 4 Statistics of normalized modal frequencies under weak wind and typhoon conditions

Mode	Frequency range (Hz)	Average frequency (Hz)	Standard deviation ( $\times 10^{-3}$ Hz)	Variance (%)	Relative variation (%)
1st	0.159-0.172	0.1651	2.878	1.74	7.87
2nd	0.216-0.230	0.2273	2.393	1.06	6.16
3rd	0.251-0.271	0.2614	2.449	0.94	7.65
4th	0.285-0.292	0.2894	1.408	0.48	2.42
5th	0.298-0.303	0.2999	0.845	0.28	1.67
6th	0.308-0.330	0.3186	4.346	1.36	6.91
7th	0.351-0.369	0.3602	2.622	0.73	5.00
8th	0.369-0.375	0.3730	1.138	0.31	1.61

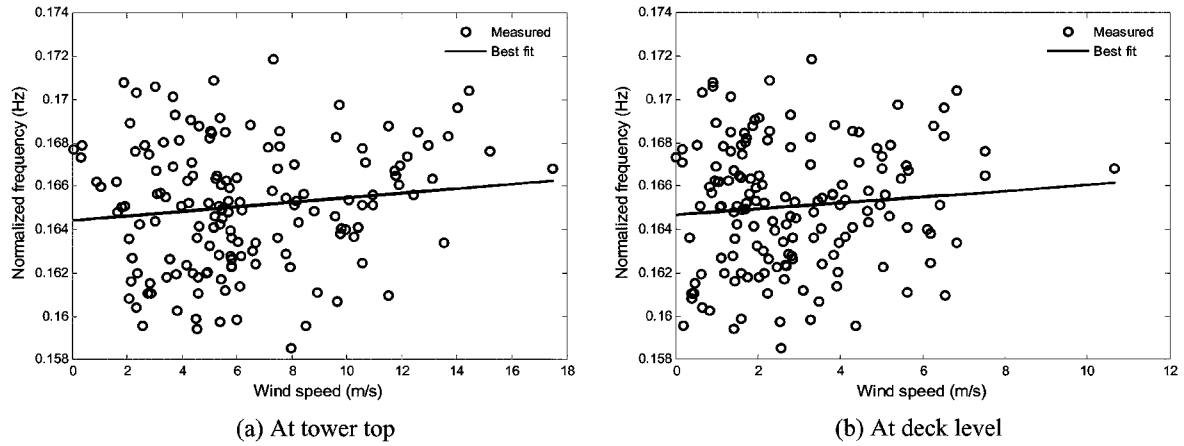


Fig. 10 Correlation between normalized modal frequency and wind speed for 1st mode

normalized frequency versus wind speed for the 1st and 4th modes, respectively. It is observed that the wind speed-frequency plotting is rather scattered and no apparent pattern exists. As made by other researchers (Abe, *et al.* 2000, Chen, *et al.* 2004), a linear regression analysis between the normalized frequency,  $f$ , and the wind speed,  $U$ , is performed by assuming

$$f = \beta_0 + \beta_1 U \quad (2)$$

where the regression coefficients  $\beta_1$  and  $\beta_0$  are obtained by the least-squares method as

$$\beta_1 = \frac{S_{fU}}{S_{UU}} \quad (3)$$

$$\beta_0 = \bar{f} - \beta_1 \bar{U} \quad (4)$$

where  $S_{fU}$  is the covariance between the normalized frequency and wind speed sequences;  $S_{UU}$  is the variance of the measured wind speed sequence;  $\bar{U}$  and  $\bar{f}$  are the means of the measured wind speed

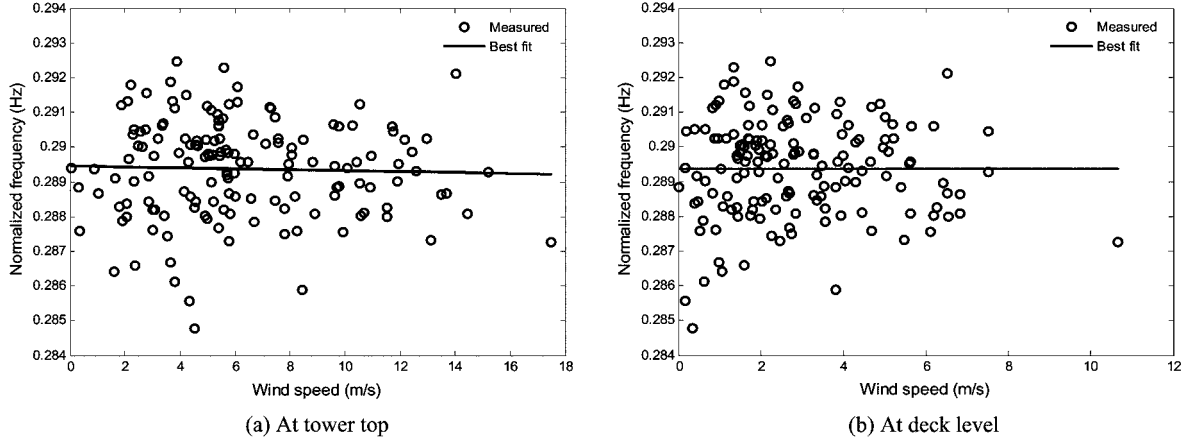


Fig. 11 Correlation between normalized modal frequency and wind speed for 4th mode

and normalized frequency sequences, respectively. In addition, the correlation coefficient,  $R$ , between the measured wind speed and normalized frequency sequences is obtained by

$$R = \frac{S_{fU}}{\sqrt{S_{ff}} \cdot \sqrt{S_{UU}}} \quad (5)$$

where  $S_{ff}$  is the variance of the normalized frequency sequence.

Table 5 summarizes the expressions of linear regression functions and the correlation coefficients of the modal frequency versus wind speed at tower top and deck level, respectively. Most of the regression functions have a positive slope, showing that the modal frequency slightly increases with wind speed in statistical sense; however, a trend of decrease in modal frequency with wind speed is also observed for some modes. The plot of the modal frequency versus wind speed is highly scattered. The correlation coefficients are less than 0.32 for all the 8 modes, implying that the correlation between the modal frequency

Table 5 Summary of linear regression models and correlation analysis

Mode	Correlation between normalized modal frequency and wind speed $f$ : frequency (Hz), $U$ : hourly-average wind speed (m/s)			
	Wind speed at tower top		Wind speed at deck level	
	Regression function	$R$	Regression function	$R$
1st	$f = 0.1644 + 0.1065 \times 10^{-3} U$	0.129	$f = 0.1647 + 0.1372 \times 10^{-3} U$	0.091
2nd	$f = 0.2244 + 0.2402 \times 10^{-3} U$	0.317	$f = 0.2247 + 0.4355 \times 10^{-3} U$	0.305
3rd	$f = 0.2607 + 0.1075 \times 10^{-3} U$	0.158	$f = 0.2610 + 0.1333 \times 10^{-3} U$	0.106
4th	$f = 0.2895 - 0.0132 \times 10^{-3} U$	-0.033	$f = 0.2894 + 0.0010 \times 10^{-3} U$	0.001
5th	$f = 0.3000 - 0.0129 \times 10^{-3} U$	-0.053	$f = 0.3000 - 0.0328 \times 10^{-3} U$	-0.075
6th	$f = 0.3168 + 0.2820 \times 10^{-3} U$	0.232	$f = 0.3179 + 0.2319 \times 10^{-3} U$	0.104
7th	$f = 0.3600 + 0.0354 \times 10^{-3} U$	0.047	$f = 0.3602 + 0.0005 \times 10^{-3} U$	0.001
8th	$f = 0.3730 + 0.0095 \times 10^{-3} U$	0.029	$f = 0.3729 + 0.0391 \times 10^{-3} U$	0.066

and wind speed is very weak. Therefore the significance of correlation in the linear regression models is further assessed.

The significance of correlation is tested through hypothesis testing on the regression coefficient  $\beta_1$ . The hypothesis of interest is the null hypothesis  $H_0 : \beta_1 = 0$  versus the alternative  $H_1 : \beta_1 \neq 0$ . If the testing result shows the acceptance of the null hypothesis  $H_0$ , it means that the regression coefficient  $\beta_1$  is equal to zero in statistical sense and therefore the correlation is of no significance. The hypothesis testing is conducted by evaluating the  $F$ -statistic (Rencher 2002)

$$F = \frac{SSR \times (m - 2)}{SSE} \tag{6}$$

in which

$$SSR = \sum_{i=1}^m [\hat{f}(i) - \bar{f}]^2 \tag{7}$$

$$SSE = \sum_{i=1}^m [f(i) - \hat{f}(i)]^2 \tag{8}$$

where  $f(i)$  is the observed (normalized) frequency;  $\hat{f}(i)$  is the predicted (normalized) frequency by the regression models;  $\bar{f}$  is the mean of the observed (normalized) frequency sequence; and  $m = 155$  is the data sample size.

The statistic  $F$  complies with the  $F_{1, m-2}$ -distribution when the null hypothesis  $H_0 : \beta_1 = 0$  is true.  $H_0$  will be rejected if  $F > F_{\alpha, 1, m-2}$  where  $F_{\alpha, 1, m-2}$ , that can be obtained from the  $F$ -table (Rencher 2002), is the critical value with a confidence level of  $1-\alpha$ . The acceptance of the null hypothesis  $H_0$  means that the correlation is of no significance, whereas the rejection of  $H_0$  implies that the correlation is of significance. Table 6 shows the values of the  $F$ -statistic and its critical lowest value for acceptance of the null hypothesis for all the 8 modes. It is seen that the  $F$  values are larger than  $F_{\alpha, 1, m-2}$  only for the 2nd and 6th modes, indicating the rejection of the null hypothesis  $H_0$  for the regression models of these two modes and the acceptance of the null hypothesis  $H_0$  for the regression models of other modes. As the null hypothesis  $H_0$  ( $\beta_1 = 0$  in statistical sense) is accepted for the majority of the modes, it is concluded that the correlation of the regression models is insignificant.

Table 6 Results of hypothesis testing

Mode	$F$ -statistic		$F_{\alpha, 1, m-2}$ (significant level = 1-0.05)
	Regression function of wind speed at tower top	Regression function of wind speed at deck level	
1st	2.5367	1.2507	3.9034
2nd	10.9721	12.5985	3.9361
3rd	2.6586	3.3034	3.9307
4th	0.1588	0.1927	3.9046
5th	0.4112	0.5095	3.9051
6th	7.7020	8.4638	3.9102
7th	0.3309	0.4129	3.9038
8th	0.1270	0.1580	3.9034

## 5. Conclusions

In this study, a method of evaluating wind-induced modal variability using long-term monitoring data has been proposed and applied to quantitatively analyze the wind-frequency correlation of the cable-stayed Ting Kau Bridge based on one-year measurement data. As temperature is the critical source causing modal variability, the measured modal frequencies and temperatures under weak wind conditions are first obtained to formulate temperature-frequency correlation models making use of ANN technique. Before the modal frequency and wind measurement data obtained under both weak wind and typhoon conditions are utilized for wind-frequency correlation analysis, the established ANN models are applied to remove temperature effect on the measured modal frequencies by normalizing them to a reference temperature. Then the normalized modal frequencies in conjunction with the wind measurement data are used to evaluate the wind-induced modal variability through statistical and correlation analyses. While the present study was purposed to separate the effects of temperature and wind on modal frequencies, the modeling of simultaneous effects of the two environmental factors on modal frequencies can be made by formulating multi-variate regression models with both temperature and wind speed as the model input.

The application of the proposed method to the cable-stayed Ting Kau Bridge comes to the following conclusions: (i) the influence of wind on modal frequencies is not as significant as the temperature effect; (ii) the temperature-frequency correlation can be satisfactorily represented by ANN models; (iii) there is an overall decrease in modal frequency with temperature for all the identified modes; (iv) the modal frequencies are observed to slightly increase with the increase of wind speed for the majority of the identified modes; and (v) both the correlation coefficients and hypothesis testing show that the correlation between modal frequency and wind speed is very weak and of no significance.

## Acknowledgements

The work described in this paper was supported by a grant from the Research Grants Council of the Hong Kong Special Administrative Region, China (Project No. PolyU 5142/04E). The writers wish to thank the Hong Kong SAR Government Highways Department, especially Ir. Dr. K.Y. Wong, Ir. W.Y.K. Chan and Ir. K.L.D. Man, for providing support to this research. Appreciation also goes to Prof. M.L. Wang at University of Illinois at Chicago for his valuable comments.

## References

- Abdel Wahab, M. and De Roeck, G. (1997), "Effect of temperature on dynamic system parameters of a highway bridge", *Struct. Eng. Int.*, **7**, 266-270.
- Abe, M., Fujino, Y., Yanagihara, M. and Sato, M. (2000), "Monitoring of Hakucho suspension bridge by ambient vibration measurement", *Nondestructive Evaluation of Highways, Utilities, and Pipelines IV*, A.E. Aktan and S.R. Gosselin (eds.), SPIE, Bellingham, Washington, USA, **3995**, 237-244.
- Adeli, H. (2001), "Neural networks in civil engineering: 1989-2000", *Computer-Aided Civ. Infrastruct. Eng.*, **16**, 126-142.
- Alampalli, S. (2000), "Effects of testing, analysis, damage, and environment on modal parameters", *Mech. Sys. Signal Proc.*, **14**, 63-74.
- Bolton, R., Stubbs, N., Park, S., Choi, S. and Sikorsky, C. (2001), "Documentation of changes in modal properties

- of a concrete box-girder bridge due to environmental and internal conditions”, *Computer-Aided Civ. Infrastruct. Eng.*, **16**, 42-57.
- Chen, J., Xu, Y. L. and Zhang, R. C. (2004), “Modal parameter identification of Tsing Ma suspension bridge under typhoon Victor: EMD-HT method”, *J. Wind Eng. Ind. Aerodyn.*, **92**, 805-827.
- Cornwell, P., Farrar, C. R., Doebling, S. W. and Sohn, H. (1999), “Environmental variability of modal properties”, *Experimental Techniques*, **23**, 45-48.
- De Roeck, G. and Maeck, J. (2002), “Influence of traffic on modal properties of bridges”, *Proceedings of the 1st European Workshop on Structural Health Monitoring*, D.L. Balageas (ed.), DEStech Publications, Lancaster, Pennsylvania, USA, 989-998.
- Doebling, S. W., Farrar, C. R. and Prime, M. B. (1998), “A summary review of vibration-based damage identification methods”, *Shock Vib. Digest*, **30**, 91-105.
- Farrar, C. R., Doebling, S. W., Cornwell, P. J. and Straser, E. G. (1997), “Variability of modal parameters measured on the Alamosa Canyon Bridge”, *Proceedings of the 15th International Modal Analytical Conference*, Society for Experimental Mechanics, Bethel, Connecticut, USA, 257-263.
- Farrar, C. R. and Jauregui, D. A. (1998), “Comparative study of damage identification algorithms applied to a bridge: I. experiment”, *Smart Mater Struct.*, **7**, 704-719.
- Hegazy, T., Fazio, P. and Moselhi, O. (1994), “Developing practical neural network applications using backpropagation”, *Microcomputers in Civil Engineering*, **9**, 145-159.
- Kim, C. Y., Jung, D. S., Kim, N. S. and Yoon, J. G. (2001), “Effect of vehicle mass on measured dynamic characteristics of bridge from traffic-induced vibration test”, *Proceedings of the 19th International Modal Analysis Conference*, Society for Experimental Mechanics, Bethel, Connecticut, USA, 1106-1111.
- Kim, J. T., Yun, C. B. and Yi, J. H. (2003), “Temperature effects on frequency-based damage detection on plate-girder bridges”, *KSCE J. Civil Eng.*, **7**, 725-733.
- Kim, J. T., Yun, C. B. and Yi, J. H. (2004), “Temperature effects on modal properties and damage detection in plate-girder bridges”, *Advanced Smart Materials and Structures Technology*, F.-K. Chang, C.B. Yun and B.F. Spencer, Jr. (eds.), DEStech Publications, Lancaster, Pennsylvania, USA, 504-511.
- Ko, J. M. and Ni, Y. Q. (2005), “Technology developments in structural health monitoring of large-scale bridges”, *Eng. Struct.*, **27**, 1715-1725.
- Ko, J. M. and Ni, Y. Q. (2007), “Uncertainty in bridge structural health monitoring: quantification and elimination”, submitted to *The 3rd International Conference on Structural Health Monitoring of Intelligent Infrastructure*, 14-16 November 2007, Vancouver, Canada.
- Ko, J. M., Wang, J. Y., Ni, Y. Q. and Chak, K. K. (2003), “Observation on environmental variability of modal properties of a cable-stayed bridge from one-year monitoring data”, *Struct. Health Monitor.*, F.-K. Chang (ed.), DEStech, Lancaster, Pennsylvania, USA, 467-474.
- Link, M., Weiland, M. and Yu, F. (2002), “Modal analysis of railway bridge hangers using artificial and ambient excitation”, *Journal De Physique IV*, **12**, 101-110.
- Lloyd, G. M., Wang, M. L. and Singh, V. (2000), “Observed variations of mode frequencies of a prestressed concrete bridge with temperature”, *Proceedings of the 14th Engineering Mechanics Conference*, J.L. Tassoulas (ed.), ASCE, Reston, Virginia, USA (CD-ROM).
- Londono, N. A. and Lau, D. T. (2003), “Variability of dynamic properties from Confederation Bridge monitoring data”, *Struct. Health Monitor. Intell. Infrastruct.*, Z. S. Wu and M. Abe (eds.), A. A. Balkema, Lisse, The Netherlands, 543-550.
- Mahmoud, M., Abe, M. and Fujino, Y., “Analysis of suspension bridge by ambient vibration measurement using time domain method and its application to health monitoring”, *Proceedings of the 19th International Modal Analytical Conference*, Society for Experimental Mechanics, Bethel, Connecticut, USA, 504-510.
- Ni, Y. Q., Fan, K. Q., Zheng, G. and Ko, J. M. (2005a), “Automatic modal identification and variability in measured modal vectors of a cable-stayed bridge”, *Struct. Eng. Mech.*, **19**, 123-139.
- Ni, Y. Q., Hua, X. G., Fan, K. Q. and Ko, J. M. (2005b), “Correlating modal properties with temperature using long-term monitoring data and support vector machine technique”, *Eng. Struct.*, **27**, 1762-1773.
- Olson, S. E., DeSimio, M. P. and Derriso, M. M. (2005), “Structural health monitoring incorporating temperature compensation”, *Struct. Health Monitor. 2005*, F.-K. Chang (ed.), DEStech, Lancaster, Pennsylvania, USA, 1635-1642.

- Peeters, B., Maeck, J. and De Reock, G. (2001), "Vibration-based damage detection in civil engineering: excitation sources and temperature effects", *Smart Mater. Struct.*, **10**, 518-527.
- Pines, D. J. and Aktan, A. E. (2002), "Status of structural health monitoring of long-span bridges in the United States", *Progress in Structural Engineering and Materials*, **4**, 372-380.
- Rencher, A. C. (2002), *Methods of Multivariate Analysis*, 2nd edition, John Wiley, New York, USA.
- Roberts, G. P. and Pearson, A. J. (1996), "Dynamic monitoring as a tool for long span bridges", *Bridge Management 3: Inspection, Maintenance, Assessment and Repair*, J. E. Harding, G. E. R. Parke and M. J. Ryall (eds.), E&FN Spon, London, UK, 704-711.
- Rohrman, R. G., Baessler, M., Said, S., Schmid, W. and Ruecker, W. F. (2000), "Structural causes of temperature affected modal data of civil structures obtained by long time monitoring", *Proceedings of the 18th International Modal Analytical Conference*, Society for Experimental Mechanics, Bethel, Connecticut, USA, 1-7.
- Sohn, H., Dzwonczyk, M., Straser, E. G., Kiremidjian, A. S., Law, K. H. and Meng, T. (1999), "An experimental study of temperature effect on modal parameters of the Alamosa Canyon Bridge", *Earthq. Eng. Struct. Dyn.*, **28**, 879-897.
- Sohn, H., Farrar, C. R., Hemez, F. M., Shunk, D. D., Stinemates, D. W., Nadler, B. R. and Czarnecki, J. J. (2004), "A review of structural health monitoring literature: 1996-2001", *Research Report No. LA-13976-MS*, Los Alamos National Laboratory, Los Alamos, New Mexico, USA.
- Xia, Y., Hao, H., Zanardo, G. and Deeks, A. (2006), "Long term vibration monitoring of an RC slab: temperature and humidity effect", *Eng. Struct.*, **28**, 441-452.
- Wenzel, H., Veit, R. and Tanaka, H. (2005), "Damage detection after condition compensation in frequency analyses", *Structural Health Monitoring 2005*, F.-K. Chang (ed.), DEStech, Lancaster, Pennsylvania, USA, 627-633.
- Wong, K. Y. (2004), "Instrumentation and health monitoring of cable-supported bridges", *Struct. Control Health Monitor.*, **11**, 91-124.
- Worden, K., Sohn, H. and Farrar, C. R. (2002), "Novelty detection in a changing environment: regression and interpolation approaches", *J. Sound Vib.*, **258**, 741-761.
- Zhang, Q. W., Fan, L. C. and Yuan, W. C. (2002), "Traffic-induced variability in dynamic properties of cable-stayed bridge", *Earthq. Eng. Struct. Dyn.*, **31**, 2015-2021.
- Zhou, H. F., Ni, Y. Q. and Ko, J. M. (2007), "Eliminating temperature effect in structural damage alarming using auto-associative neural networks", submitted to *The 6th International Workshop on Structural Health Monitoring*, 11-13 September 2007, Stanford, California, USA.